Fishtail effect in the magnetization of superconducting $R\mathrm{Ba_2Cu_3O_{7-\delta}}$ (R=Y,Nd,Yb) and $\mathrm{Y_2Ba_4Cu_8O_{16}}$ single crystals

M. Werner, F. M. Sauerzopf, and H. W. Weber
Atominstitut der Österreichischen Universitäten, A-1020 Vienna, Austria

A. Wisniewski
Institute of Physics, Polish Academy of Sciences, PL-02668 Warszawa, Poland
(Received 1 June 1999)

The second peak in the magnetization (fishtail) of superconducting single crystals was investigated for magnetic fields parallel to the crystallographic c axis. Several $R\mathrm{Ba_2Cu_3O_{7-\delta}}$ crystals and one $\mathrm{Y_2Ba_4Cu_8O_{16}}$ crystal were studied by various experimental techniques. We observe a similar behavior of the fishtail effect independent of the initial state of our samples. In order to assess the dependence of the fishtail on the defect size and concentration, the defect structure was modified by reactor neutron irradiation and additional annealing treatments. Our results emphasize the important role of normal conducting regions, which are created by clustering of defects, typically of oxygen vacancies. Evidence in favor of strong pinning is presented.

I. INTRODUCTION

Since the discovery of the high-temperature superconductors (HTSC's) one feature in the magnetization curves of these materials has been especially controversial in the literature: the fishtail effect. This effect, which is also called the *second peak effect*, refers to an increase of the critical current density J_c with increasing magnetic field. An incredible amount of publications dealing with this phenomenon has been published, but the interpretation of the effect still is rather controversial. Therefore, a closer look at the most reliable experimental studies and plausible theoretical interpretations seems to be necessary. The various concepts will be presented in a survey of the field in Sec. II. Then, details of our own experiments will be given in Sec. III, where we describe our samples, measurement procedures, and aspects of the evaluation process related to the determination of the critical current density. In order to show that the effect is widely insensitive to the sample preparation, we use several types of HTSC crystals, produced by various methods, and measure them in different experimental setups. Additionally, we modify the pinning defect structure in some crystals by reactor neutron irradiation to low fluences and by annealing. The results are presented in Sec. IV, together with a critical discussion of the standard interpretations of the fishtail effect. We check the currently available models with respect to our own data and find that a consistent explanation is not yet available, although many features of the effect can be explained in a qualitative way.

II. SUMMARY OF PREVIOUS WORK

An increase of the critical current density with increasing field was already observed in some low-temperature superconducting materials (LTSC), where at least three different mechanisms were identified depending on the nature of the defects.[1]

In NbTi, a regular array of normal conducting precipitates causes *temperature independent* peaks whenever the flux line lattice parameter $a_0 \simeq 1.07\sqrt{\Phi_0/B}$ is equal to the distance between the defects. This effect has originally been called the *matching effect*.[2]

Another possibility for a peak effect in conventional type-II superconductors, e.g., in PbIn or PbNa alloys, is the existence of a second superconducting phase, with lower superconducting parameters (upper critical field H_{c2}, critical temperature T_c).[3] In this case, the induction where the maximum critical current density J_c occurs B_{max}, depends on temperature.

A third mechanism which often led to sharp peaks near H_{c2} in weakly pinning superconductors is due to a very small shear modulus of the flux line lattice c_{66}, which actually vanishes at $H_{c2}(T)$. The resulting peak effect in the critical current density can be understood in terms of the collective-pinning theory.[4] A particularly complete study of this effect was made by Meier-Hirmer *et al.*[5] using radiation-induced point defects in V_3Si single crystals, which varied in their concentration by more than three orders of magnitude. They found sharp peaks developing near H_{c2} in the initial state and at low defect concentrations, which broadened and shifted to lower fields with increasing defect density, and finally vanished when even more defects were introduced. Very good agreement with the static collective-pinning theory was obtained at low defect densities. At higher defect concentrations the behavior was attributed to plastic flow of the flux lines.

Since the discovery of the fishtail feature in HTSC's, where it is predominantly observed in the $R\mathrm{Ba_2Cu_3O_{7-\delta}}$-system, several explanations have been proposed, relying on both static and dynamic mechanisms. Static interpretations explain the effect by an increase of the macroscopic pinning force, in agreement with one or more of the mechanisms observed in LTSC's. The dynamic models are based on the field dependence of the flux-creep rate, but still assume that the unrelaxed current density decreases monotonously with B.

The first attempt to explain the fishtail feature[6] in

$YBa_2Cu_3O_{7-\delta}$ (Y-123) single crystals was made within the static interpretation. In this picture, small oxygen-deficient regions in the sample turn normal conducting at a temperature far below the bulk critical temperature T_c. This produces additional pinning centers in increasing external fields, which may act discretely at low densities, but become multiply connected at higher defect density and divide the crystal into ''grains,'' thereby leading to the strong suppression of J_c in fields above the second peak. In connection with this model, others[7,8] were formulated, which basically argue via oxygen deficiency and granularity. The strongest argument in favor of these explanations is that they allow one to understand the temperature dependence of the peak field H_{max}, i.e., the field where the maximum of J_c is observed. Very soon, however, the first paper appeared[9] reporting that the peak did not disappear even after long oxygenation treatments, when the oxygen content was supposed to be optimized. The concept of granularity also had to be dropped, when Gordeev *et al.*[10] showed fishtail behavior in a transport measurement.

Another possibility within the static approach refers to the microscopic defect structure of single crystals. The so-called ''matching theory''[11] suggested that the flux line lattice (FLL) parameter a_0 would optimally match the random defect structure at some specific magnetic field, i.e., H_{max}. However, while this idea seems to be quite plausible from its equivalence to the matching effect in LTSC's, some mathematical modeling would be necessary to ascertain its applicability.

Other groups proposed that the fishtail was affected by the sample shape[12,13] or that the second peak was based on a softening of the vortex lattice,[14] which would allow a better adaption of vortices to the defect structure, equivalent to the same argument in LTSC's. This effect could lead to an increase of the macroscopic pinning force, but is also based on plausibility arguments, without mathematical backing.

Although a lot of effort has been put into the approaches mentioned so far, none of them succeeded to explain the origin of the fishtail effect consistently. Thus, the dynamic properties of HTSC's were studied more intensely. In this case the time-dependent shielding current density J_S replaces the critical current density J_c. Very early, the normalized relaxation rate of flux creep was investigated in the framework of the collective-pinning theory[15,16] in the form given by Blatter *et al.*[17] They suggested that the existence of the second peak was related to a nonequilibrium crossover from the single vortex regime to collective pinning of vortex bundles. The magnetization is very low at low fields because of the higher relaxation rate S. Therefore, in this model the normalized relaxation rate S is expected to be the mirror image of the magnetization curve.

This model was soon questioned[18] because the minimum of the normalized relaxation rate S is usually observed at fields significantly below the position of the magnetization maximum, and because samples with and without the fishtail feature show qualitatively the same relaxation behavior. In Refs. 18 and 19 the explanation of the fishtail effect is based on a change of the elastic properties of the vortex lattice.

In another approach, a universal behavior[20–22] in the flux-creep rate as a function of the reduced external field ($h = H/H_{max}$) was found from vibrating-sample magnetometer measurements. The scaling field H_{max} is the position of the second maximum. From these scaled curves, three regimes of distinctly different behavior in the vortex dynamics were defined, which led to the assumption of three basically different mechanisms of flux pinning.

The dynamic aspects of the problem are the basis for the next attempt to explain the feature.[23] From torque measurements the so-called ''true'' critical current density was calculated within the generalized inversion scheme.[24] This current does not increase with increasing field, which is considered as a proof for the validity of the dynamic approach. The authors suggest that the fishtail is only due to a very high relaxation rate at low fields. From their model calculations and experimental observations they find no crossover of pinning regimes as concluded in Ref. 15. This is also confirmed by the observation of a fishtail in a Pb-irradiated $DyBa_2Cu_3O_{7-\delta}$ single crystal,[25] since the introduction of strong pinning centers should shift the transition from three- to one-dimensional pinning (in terms of Ref. 15) and therefore would remove the fishtail, if it were caused by a crossover between pinning regimes in the described way.

A recent paper[26] relates the peak effect to an uncorrelated statistically distributed defect structure, which pins more strongly when the flux line lattice softens. From the anisotropy of the magnetization with respect to the external field the authors argue that the fishtail is present independently of the orientation of the applied field to the $\hat{c}$ axis, while the peak correlated to the twin structure disappears, if the misalignment angle α between field and crystallographic $\hat{c}$ axis is bigger than a certain angle ($\simeq 8°$). As found in a previous paper,[27] the fishtail broadens and H_{max} is shifted to higher values with increasing α. Fully oxygenized twin-free single crystals did not exhibit any peak. By reducing the oxygen content the authors changed the defect structure (density and/or size) and investigated the resulting J_c values. The peak develops first at high fields near the irreversibility field. With increasing oxygen deficiency δ the peak broadens, becomes higher and shifts to lower fields. For external fields above the peak field H_{max}, the curves of J_c merge indicating an independence of J_c on the defect density. In analogy to the interpretation of older data on V_3Si,[5,28] they conclude that for fields below the peak the static collective-pinning theory qualitatively explains the field dependence of the current density, while above H_{max} the saturation behavior gives experimental evidence for plastic interactions, in contradiction to the collective model. In between, a continuous transition from elastic to plastic interaction takes place. This publication provides strong arguments that the peak is due to pinning by clusters of oxygen vacancies, in accordance with Refs. 29 and 30, and excludes a significant contribution from single vacancies.

Two different flux-creep mechanisms above and below the peak were also inferred to explain the dependence of the pinning potential U on the critical current density J_c by experiments using local Hall probe arrays.[31] In particular, below the peak the collective creep theory can be applied, while above the data show good agreement with the dislocation mediated mechanism of plastic creep.[32] Hence, the authors conclude that the origin of the fishtail effect is a crossover from elastic to plastic creep. For the temperature

TABLE I. Sample overview.

Sample code	Type	Dimension (mm^3)	Mass (mg)	T_C (K)	Experiments [a]	Treatment [b]
D208-12 [c]	Y-123	$0.843\times0.679\times0.065$	0.251(5)	89.91	S	nna
D208-13 [c]	Y-123	$0.783\times0.41\times0.096$	0.207(3)	91.1	S	
M3944 [c]	Y-123	$1.06\times0.644\times0.313$	1.398(9)	83.1	S, M, H	nNN
Götti [d]	Yb-123	$1.576\times0.608\times0.0381$	0.265(4)	89.11	S, T, M	
Gött2 [d]	Yb-123	$1.578\times0.75\times0.052$	0.503(4)	88.93	S	
Nd15 [e]	Nd-123	$1.517\times0.4375\times0.185$		93.1	S, M	
Pla1 [f]	Y-124	$0.8\times0.46\times0.07$		78.88	S	nNa

[a]S indicates SQUID, T is Torque, M is Magneto-optics, H is Hall probe array.

[b]n indicates low fluence neutron irradiation $10^{20}m^{-2}$, N is high fluence neutron irradiation $\geqslant10^{21}m^{-2}$, a is annealing, 250 °C, 8 h.

[c]B. W. Veal, Argonne National Laboratory, USA.

[d]K. Winzer, University of Göttingen, Germany.

[e]M. Murakami, ISTEC, Japan.

[f]J. Karpinski, ETH Zürich, Switzerland.

dependence of the peak, they reported $B_{\max}\propto[1-(T/T_c)^4]^{1.4}$.

The reversible production or removal of the fishtail peak was also demonstrated by varying the parameters of the oxygenation process in ultrapure crystals[29,33,34] with a purity of better than 99.995 at. %. Annealing a crystal under high-pressure oxygen removes the second peak. Reannealing the same crystal according to the standard method under one bar oxygen reinstalls the fishtail peak. According to Lindemer *et al.*[35] the overall oxygen content is the same for both annealing treatments ($\delta=0.09$). Thus, Erb *et al.* conclude that only a locally altered oxygen distribution or oxygen ordering must be responsible for this effect. This can be interpreted as clustering of oxygen vacancies, which act as additional pinning centers when they become normal conducting (cf. Ref. 6). They conclude that in high-quality single crystals of $YBa_2Cu_3O_{7-\delta}$ the fishtail effect is due to clusters of oxygen vacancies. These clusters will always be present in less pure single crystals due to cation impurities, which cause clustering of defects even under high-pressure oxygenation conditions. This work very convincingly describes the defect type responsible for the fishtail effect in very pure crystals. We intend to complement this work in the range of impure systems in an attempt to identify the common underlying mechanism of the vortex-defect interaction and placing less emphasis on the identification of specific defects, which cause the fishtail effect.

We will show, that the fishtail effect is consistent with a crossover between pinning regimes, but that the currently considered models cannot fully explain the results, as already mentioned in another context in Ref. 30.

III. EXPERIMENTAL DETAILS

A. Samples

Several $YBa_2Cu_3O_{7-\delta}$ single crystals were investigated.[36] Some of their physical properties and the sample codes are summarized in Table I. The crystallographic quality of all samples was studied by x-ray diffraction and found to be excellent. Furthermore, magneto-optical images showed uniform flux penetration patterns, which indicates homogeneous current paths and a good sample quality. One of the Y-123 crystals is oxygen deficient, *M3944* with $\delta\simeq0.2$ and $T_c=83.1$ K. Additionally, other types of crystals were included in the experiments, a $NdBa_2Cu_3O_{7-\delta}$ (Nd-123), two $YbBa_2Cu_3O_{7-\delta}$ (Yb-123) and a $Y_2Ba_4Cu_8O_{16}$ (Y-124) single crystal. In a previous study we have checked the influence of different contaminations from the crucible on the fishtail effect of Y-123 crystals, but could not find a significant dependence on the crucible material (Al_2O_3 or Au), even though the substitution of Al and Au has significantly different metallurgical consequences. For the $RBa_2Cu_3O_{7-\delta}$ crystals, oxygen deficiency seems to be the dominating type of defect, maybe with a contribution by the Nd-Ba antisite-defect in Nd-123 and a significant contribution from twinning. Neither oxygen deficiency nor twinning exist in the Y-124 system,[37] and, indeed, the hysteresis in ultrapure crystals grown in $BaZrO_3$ crucibles is extremely small, down to very low temperatures.[38] Our crystal was grown in a Y_2O_3 crucible and showed a strong fishtail effect even at $T=5$ K. The identification of the defects responsible for flux pinning in all these systems is still difficult. Even the extremely thorough characterization of ultrapure Y-123 single crystals by Erb *et al.* (e.g., Ref. 29) led only to the identification of oxygen clusters as pinning relevant defects, but did not provide sufficient data on the resulting defect size and density. Despite all the progress in the field the relevant defects cannot be analyzed by microscopical methods. On the other hand, we can be sure that a wide variety of possible defects is covered by the set of samples selected for the present study, which is further widened by the well-defined variation of the defect structure after neutron irradiation.

B. Irreversibility line and critical current density

For all samples, the magnetic moment as a function of field and temperature was measured in a superconducting quantum interference device (SQUID). Additionally, torque magnetometry, magneto-optical investigations (both at the Vrije Universiteit Amsterdam) and local Hall-probe measurements (Bar Ilan University) were applied in some cases in order to check the reliability of the results (see Table I). A comparative study of the various setups and experimental methods was presented in Ref. 39. The main experimental

work was carried out in Vienna, where all the crystals were investigated by SQUID magnetometry in the 1 and 8 T setups at temperatures from 5 to 80 K. The magnetic moments at fixed temperatures with the external magnetic field aligned parallel to the crystallographic $\hat{c}$ axis, were measured and the shielding current densities J_s in the *ab* planes were calculated.

Furthermore, the temperature dependence of the irreversibility line (IL) was obtained by zero-field-cooling, measurements in various fields up to 8 T. The experimental assessment of the irreversibility line is affected by the ''experimental time window'' and the resolution of the experimental technique employed, because of the high relaxation in the HTSC's and the necessary criterion for defining $J_s=0$.

The definition of the irreversibility point in our work is based on a simple but very accurate method,[40,41,30] which takes advantage of the movement of the sample between the pickup coils in the slightly inhomogeneous field of the magnetometer. This leads to a small ''ripple field'' superimposed to the external dc field, which amounts to about 0.1% of the applied field and corresponds to a frequency of around 0.05 Hz.[42] In the reversible regime, the SQUID response is the same for both directions of the sample movement. When flux pinning sets in, characteristic distortions appear in the curves, which reflect the hysteretic behavior of the magnetization, and are history dependent. This can be parametrized by comparing the SQUID output voltages at the same sample position but for different directions of the sample movement. For measurements at constant field, the sum of squares of these differences at roughly hundreds of sample positions abruptly decreases at one specific temperature, which defines the irreversibility temperature. In this way, the $J_s=0$ criterion can be approximately defined as 10^4–10^5 Am^{-2} (depending on the sample size and the external field).[1]

The evaluation of J_s is based on an extended Bean model,[40,43] where the current density is evaluated in terms of Bean's critical-state model,[44] but the generated local self-field H_{self} and the influence of the anisotropy of the samples at different field orientations are also included to first order.

C. Neutron irradiation and annealing

In order to modify the defect structure of the material we treated selected crystals by fast neutron irradiation and annealing. It has been shown that fast neutron irradiation[45,46,30] represents a powerful tool for changing the relevant defect structure for flux pinning by the formation of large strongly pinning collision cascades and agglomerates of smaller defects. The irradiation typically leads to improved pinning properties at the expense of slightly decreasing T_c at low and intermediate fluences.

The samples were irradiated in the central core position of the TRIGA reactor in Vienna. The neutron energy spectrum and the flux density at this position are given in Ref. 47. The samples were encapsulated in small quartz tubes under normal atmosphere. During irradiation the tube was contained in a small aluminum can immersed in the cooling water of the reactor. At full reactor power the temperature of the samples rises to 50–60 °C. The resulting defect structure and its general effect on flux pinning are considered in detail in Ref. 30.

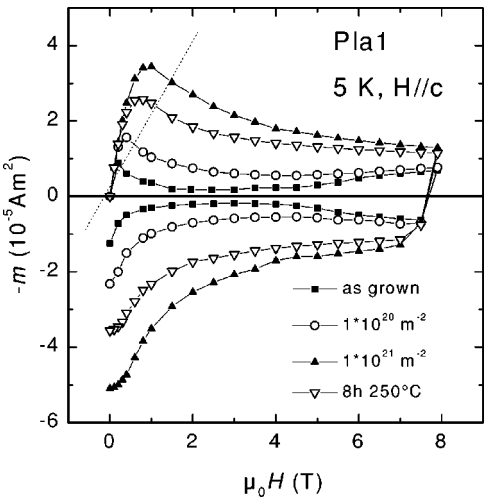

FIG. 1. Low-temperature magnetization curves of a Y-124 crystal, before and after irradiation and annealing. The dashed line indicates the position of the Bean penetration field.

Briefly, it consists of a number of strongly pinning defect cascades with a density proportional to the fast neutron fluence,[48] e.g., at a neutron fluence of 2×10^{21} neutrons/m^2($E>0.1$ MeV) the cascade density amounts to 1×10^{22} m^{-3}. The applicability of these numbers for various HTSC's can be inferred from a similar study[49] on $Bi_2Sr_2CaCu_2O_8$ single crystals. The size of the cascades is comparable to the coherence length of the HTSC's at elevated temperatures, which makes them perfectly suitable for core pinning. Also, various small defects, e.g., point defects, point defect clusters, and interstitials, are generated during the irradiation process. Some fraction of the smaller defects may agglomerate to build another type of large defects, which is also capable of strong flux pinning.

Under annealing (8 h at 250 °C, in air), the mobility of defects is strongly enhanced in the crystals, but no oxygen loss occurs at this low temperature. Thus, only the small defects and agglomerates, which can be dissolved, are affected by this treatment. Mobilized point defects migrate through the crystal until they are caught at strong defect traps, e.g., the cascade regions or twin boundaries. It has been shown[48] that the defect cascades are stable up to at least 400 °C. During annealing, the crystals remain glued onto a sample holder aluminum platelet with high vacuum grease, which is stable in air for temperatures up to 250 °C and not harmful to the samples. It has been shown consistently[30] that the removal of small defects is the dominating effect under annealing.

IV. RESULTS AND DISCUSSION

A. Defects after irradiation and annealing

The typical fishtail shape is most commonly observed in the magnetization curves. In order to give an example, data on a Y-124 single crystal at $T=5$ K are shown in Fig. 1 for various crystal treatments. A distinct fishtail is observed in the untreated and the weakly irradiated (10^{20} m^{-2},$E>0.1$ MeV) crystal, even at this low temperature. Although it is not observed after irradiation to higher fluences, it is useful for the distinction between the static and the dynamic

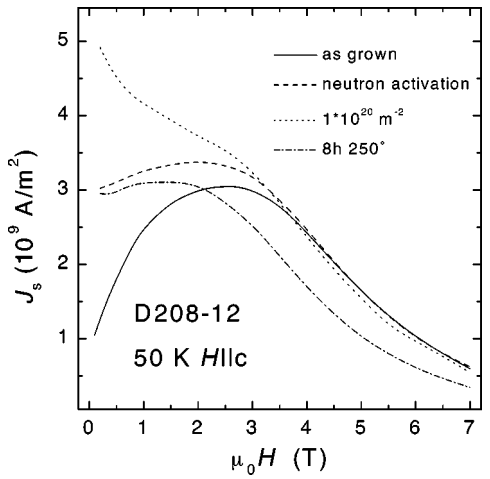

FIG. 2. Shielding current density of a Y-123 crystal [T_c (untreated) $=89.9$ K] determined from magnetization curves at $T=50$ K, before and after low fluence neutron irradiation and annealing.

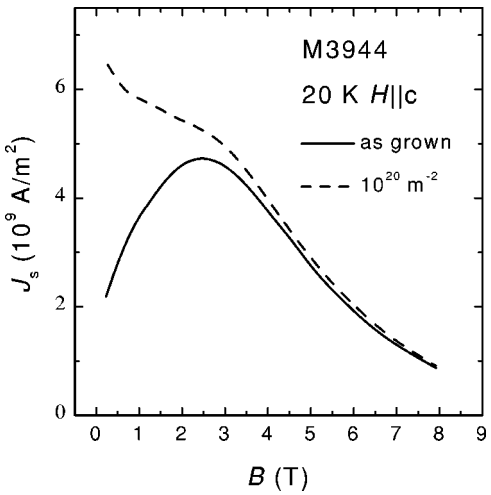

FIG. 3. Shielding current density of a Y-123 crystal [T_c (untreated) $=83.1$ K] at 20 K, before and after low fluence neutron irradiation.

interpretation of the fishtail effect. Because relaxation is comparatively weak at 5 K ($T/T_c \approx 0.06$) and cannot account for the observed effect, these data present a strong argument in favor of a static explanation of the fishtail.

The anomalous magnetization at low temperatures in our experimental window is observed only in some untreated or very lightly irradiated crystals. At higher temperatures the effect is observable in almost all measurements. With increasing fluences, the peak shifts to lower fields, where it sometimes cannot be detected in magnetic measurements (when the peak field is comparable to or lower than the Bean penetration field H^*). An example of this behavior is given in Fig. 2, where data on a Y-123 single crystal are shown. This figure nicely illustrates the dependence of the fishtail peak on the various types of defects present due to the sample treatment. The as-grown crystal shows a distinct maximum in the $J_s(H)$ dependence. After the first neutron irradiation, which was made in order to determine the gold content of the sample[50] by neutron activation analysis (NAA), strong irradiation effects were observed. Unfortunately, the associated fast neutron fluence could not be exactly determined for that irradiation position. Therefore, another irradiation followed in a position with a known fast neutron fluence (1×10^{20} m^{-2}), which is estimated to be of the same order of magnitude as that for the NAA. The results were surprising. While the effect of neutron irradiation was attributed to the typical large defect cascades until recently,[30] the density of these defects is by far too low to have a distinct effect on flux pinning at these very small fast neutron fluences. Nevertheless, the shielding current density is strongly enhanced at low fields. The second peak is still discernible after the NAA and is only visible as a small bump in the curve after the second irradiation. At high fields only a very small effect is visible. Even more interesting is the behavior after annealing the crystal at 250 °C. The fishtail reappears, although in lower fields than before, while at the same time J_s at high fields is significantly reduced. The maximum values are now of the same order as in the untreated crystal, but occur at lower fields, with a significantly smaller slope towards zero. From this, it is obvious that the effects of irradiation and annealing on the defect structure are not only counteracting each other, but that the underlying mechanisms are qualitatively different.

Another example for the effect of low fluence irradiation at intermediate temperatures is shown in Fig. 3. The very small neutron fluence significantly increases J_s at low fields and leaves it almost unchanged in the field range above the peak, which makes the peak effect almost invisible. A similar behavior has been observed in all our samples after low fluence irradiation.

According to previous work,[26,30] we can be sure that the large defect cascades introduced by neutron irradiation are by far too few at the low fluences to have a significant effect on flux pinning. Point defects only contribute in the form of clusters. These clusters can be formed either at new defect sites or at previously existing defect regions. After irradiation, we find that the increase of J_s is very large at low fields, but not significant at high fields. This provides a clue for the defect evolution under irradiation and annealing, respectively. In all present theoretical approaches, the product of the defect density and the (square of the) elementary pinning force $N_d \cdot f_p^i$ determines the influence of the defect structure on the shielding currents, where $i=1$ for the direct summation model, and $i=2$ for most other theories. It would be rather coincidental, if this factor would exactly cancel in all our experiments. Therefore, we conclude from our data that only one of the two parameters, N_d or f_p, will significantly change due to low fluence irradiation, and that this change is less important in high fields. Both alternatives, i.e., clustering of newly created defects at previously existing sites or the creation of new defects, are possible, but cannot be distinguished considering only the data after irradiation.

However, the defect evolution responsible for the data in Fig. 1 is easier to resolve from the situation after annealing. Loosely bound clusters dissolve and point defects move into stable defect sinks, which are enlarged to some extent. We, therefore, assume that under annealing the overall number of defects is reduced, and that some fraction of the previously existing defects is enlarged, i.e., their elementary pinning force is enhanced. This picture is consistent with the experimental data, if the reduction of J_s at high fields is attributed

to the *decreasing* density of pinning centers. The simultaneously increasing size of the defects is not effective for J_s, because the elementary pinning force f_p is limited by the FLL stability—this applies when the elementary pinning force is strong enough to pull a vortex from its position in the FLL. A limit of this kind is quite plausible if simple numerical calculations in the elastic theory[30,51] are considered, where the maximum distortion of the FLL due to a typical pinning force is evaluated as a function of the external field. At low fields even after annealing, enhanced values of J_s are found compared to the unirradiated crystal. They are due to the increase in f_p, i.e., to a lower density of stronger pinning centers.

After irradiation J_s showed a qualitatively different behavior from that after annealing. This allows us to decide between the two scenarios described above. The correct scenario is a minor change of the pinning center density after the low fluence irradiation accompanied by a large increase of the elementary pinning force of some of the previously existing defects. This is consistently explained by the migration of point defects to these sites. The limitation in the increase of the elementary pinning force is again set by the stability of the FLL.

B. Defect evolution and the fishtail

Following this qualitative description of the defect structure after irradiation and annealing we concentrate on the interaction between the FLL and this defect structure, in order to clarify the mechanisms leading to the observed J_s data. After the low fluence neutron irradiation, predominantly f_p is increased, which shifts the fishtail peak to lower values. The field dependence of J_s at high fields is not changed, but the same dependence now extends to lower fields. In our model, J_s in the high-field regime is dominated by the stability of the FLL. Therefore, the increase of f_p is consistent with the extension of this regime to lower fields. Below this regime, i.e., below the peak in J_s, increasing f_p means a larger maximum distortion u_0 of the FLL. This defines the fraction of actually pinning defects, which roughly should be $u_0^2\pi/a_0^2$. Therefore, increasing f_p leads to an increase of J_s in the region below the peak. The peak effect itself is in these terms explained by an increase of u_0/a_0 with B at low fields and the regime where f_p is limited by the FLL stability at high fields.

Another possible explanation for the fishtail ''peak'' is a *suppression* of J_s in the region of the minimum, which could be caused by the competitive effect of neighboring pinning centers on the flux lines. This is possible when the distortion fields caused by the pinning centers overlap. The maximum in J_s is then due to ''matching'' (in a statistical sense only), where an optimum fit of the FLL positions to the defects occurs.

The fishtail according to these models has to be due to a rather uniform defect structure, because in the presence of a highly inhomogeneous defect structure the locally different peaks would average out.

The arguments as described above refer to the static regime and are based on the conclusions drawn from Fig. 1. In the presence of thermal activation, the less stable configurations at low fields and especially in the high-field regime are much more easily thermally acivated. Therefore, our arguments explain the strong enhancement of the fishtail effect at high temperatures.

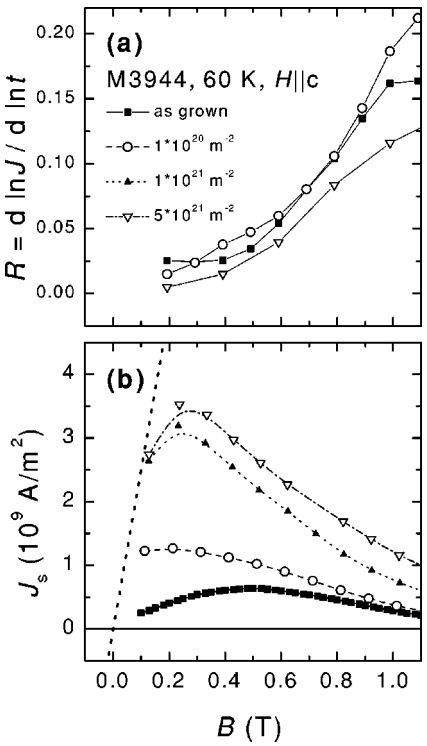

FIG. 4. The relative relaxation rate of the oxygen-deficient Y-123 crystal [T_c (untreated) $=83.1$ K] at $T=60$ K and after neutron irradiation (a) and the shielding currents as determined from magnetization measurements for the same conditions (b).

Relaxation rates from Hall measurements determined for sample M3944 are shown in Fig. 4(a). A smooth increase of the relaxation rate with field is observed at all fluences, with a possible dip only for the unirradiated crystal. It is obvious that this dip ($\lesssim 0.4$ T) occurs below the peak of the magnetization curve (~ 0.5 T) shown in Fig. 4(b). For the other treatments, no dip is visible in the relaxation rate, but a significant fishtail feature reappears after irradiation to a higher neutron fluence, at rather low fields (~ 0.5 T). Therefore, a direct correlation between the relaxation rate and the second peak cannot be observed, exactly as in other measurements on unirradiated samples. We do not have relaxation measurements on other irradiated crystals, but the shielding current densities J_s of all crystals reflect the same behavior.

A distinct peak effect is observed in J_s of the samples irradiated to a high fluence. Some care has to be taken when deciding whether this is due to an actual decrease of J_s in lower fields or is just an artifact of demagnetizing effects. J_s is calculated from the decreasing slope of the magnetization curve in this field range. Due to the averaging procedure over the field distribution in the sample[43] $J_s(B)$ might be erroneous at fields, below which the local field at the corner of the sample falls below zero. The line indicating this border is shown as the dashed line in Fig. 4(b). Clearly, our data points are above this line. In addition, the average induction in the sample would have to be around 0.5 T, in order to account for the observed low J_s, which is impossible. Therefore, the peak effect is positively identified as a true peak

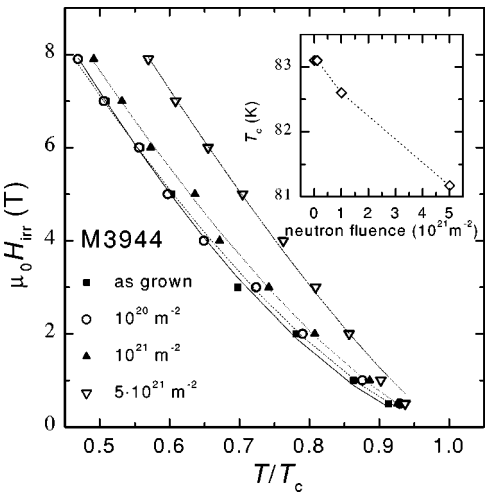

FIG. 5. The irreversibility line of the oxygen-deficient Y-123 crystal [T_c (untreated) $=83.1$ K] after sequential neutron irradiation of the sample.

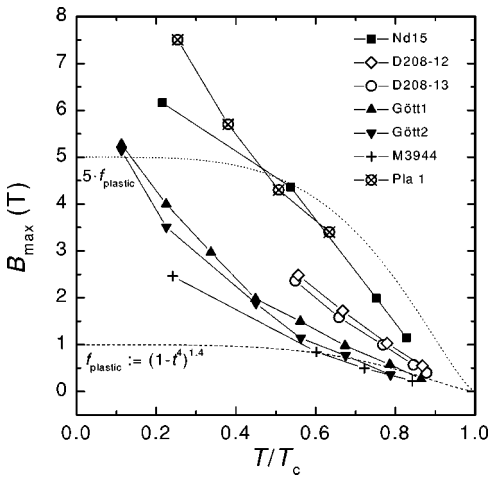

FIG. 6. The field at the peak position as a function of temperature for various untreated crystals described in Table I. For comparison, the prediction of a transition from collective pinning to plastic vortex movement (dotted line, f_{plastic}) is included.

effect of J_S, and has to be explained in our model. In the as-grown crystal, one defect structure (most likely intermediately sized clusters of O vacancies) is dominant. By the low fluence irradiation, the pinning strength of the defects is increased. At the same time, a rather inhomogeneous defect structure is created, because the number of new interstitials, which may recombine with vacancies, is rather high in the vicinity of the few defect cascades. Their density is very low ($\sim 5\times 10^{20}$ m^{-3}) and their pinning contribution can be neglected in this fluence range. For the high fluence irradiation, the density of cascades is proportionally increased and a homogeneously distributed structure of these strong pinning centers is created. This is reflected in the lowered relaxation rate, and causes the fishtail effect to reappear at lower fields and higher absolute values of J_S. It should be pointed out, that the data cannot be explained by the effect of the irradiation on T_c, which is only lowered by roughly two degrees at the highest fluence (cf. the inset in Fig. 5).

The massive impact of strong pinning centers at high neutron fluences manifests itself also in the irreversibility line (IL). The IL gives information about the pinning situation in the case of extreme thermal activation, where only the largest defects are still active pinning centers. This is illustrated in Fig. 5, again for crystal M3944, in order to allow a comparison with Fig. 4. Whereas J_s(60 K) and the fishtail effect [Fig. 4(b)] are only slightly changed by the last irradiation, the IL moves to significantly higher temperatures, in good agreement with the observed decrease of the relaxation at 60 K [see Fig. 4(a)]. The effect of lower fluence irradiation, and also of annealing, on the IL is not as unambiguous as for the current densities, and, therefore, does not allow safe conlusions. As observed before (cf. Refs. 46 and 30), neutron irradiation may lead to an increase or a decrease of the irreversibility fields, depending on the respective sample. This is also true for the annealing treatment. A plausible interpretation of these data might allow one to draw further conclusions on the defect structure in the specific samples. We refrain from doing so, because it would be quite speculative at the moment and also beyond the scope of this work.

Recent papers (e.g., Refs. 31, 26) proposed an explanation of the fishtail effect in terms of a plastic flow of the FLL. This approach is qualitatively consistent with our interpretation of the effect, but some quantitative features are not. We agree that the macroscopic pinning force is enhanced by the reduction of correlated volumes in the FLL in increasing field, but the description in terms of present collective-pinning models (e.g., Ref. 17) is not sufficient. Even though many of the experimentally observed features are explained by the collective-pinning approach, it has been shown that it does not describe the dependence of the pinning force in Y-123 crystals as a function of the density of pinning centers.[30]

A quantitative evaluation of the crossover from collective pinning to the regime of plastic vortex movement was attempted in Ref. 31, where the peak field was reported to depend on temperature through a function $f_{\mathrm{plastic}}=(1-t^4)^{1.4}$. In a comparison of this function to our data (Fig. 6) we find complete disagreement. The good fit reported in Ref. 31 is due to the fact that only high temperatures were measured in that experiment. In Ref. 26 even an upturn of the peak field at high temperatures was found for their very weakly pinning overdoped Y-123 crystals.

V. CONCLUSIONS

We compared published data and models to new data, which were obtained after neutron irradiation and annealing of various HTSC single crystals. All of the crystals showed similar features, although they differed considerably (oxygen content; $R=$Y,Nd,Yb; R-123,Y-124). None of the models in the literature is able to explain the full temperature and field dependence of the fishtail effect in our samples, although many of their basic features are consistent with the data. Especially the static collective-pinning approach, where the reduction of the correlated volume with increasing field leads to enhanced flux pinning and a crossover to a badly correlated vortex structure (plastic regime) might be useful. Nevertheless, a quantitative comparison with all the proposed models leads to inconsistencies with our data.

For example, the low-temperature field dependence of J_S (especially for the Y-124 crystal) and the missing correlation

between fishtail and relaxation behavior rule out explanations exclusively based on dynamical effects. Furthermore, the creation of additional pinning centers at high fields and temperatures can be dismissed, because it is inconsistent with the results after low fluence irradiation and annealing. Under this treatment, the fishtail effect is suppressed by the irradiation and reinstalled after annealing, which cannot be explained in this framework.

Hence, we developed a qualitative model, which is consistent with our data and the generally accepted theoretical treatment of the flux line lattice. In our approach, we do not depend on a specific type of defect, but instead describe which features of the vortex lattice and of the defect structure lead to the observed effects. This seems to be a better approach than that of many previous studies, because we observed the fishtail effect in a large variety of samples with strongly differing properties.

J_s at high fields is not significantly changed after low fluence irradiation, and the influence of annealing on J_s is qualitatively different from that of irradiation. This infers that the main effect on the shielding current density after irradiation is the increase in the elementary pinning force, which is not significant at high fields, because in this region the elementary pinning force is limited by the stability of the flux line lattice. The reduction of J_s by annealing is due to the reduced number of defects. Using this approach we find a consistent description of the fishtail effect. At low fields the normalized displacement of a flux line by the elementary pinning force u_0/a_0 is increasing, leading to a higher fraction of available pinning centers, and to increased J_s. Also, the minimum region could be due to a less stable flux line configuration because of a mismatch between the pinning defects and the flux line lattice. At high fields either is $u_0/a_0 \gtrsim 0.5$, which limits the elementary pinning force, or, alternatively, all available defects are occupied. In both cases we expect a saturation of the macroscopic pinning force, which leads to a decrease of J_s, as explained in terms of the standard models. In any case, the resulting peak effect is not only determined by a specific defect density, but also by the elementary pinning force of the defects. This leads to a disappearance of the effect in very inhomogeneous defect structures, e.g., after neutron irradiation. The fishtail can reappear when the defect structure is homogenized by subsequent annealing, or if a new dominant defect structure evolves, e.g., after high fluence irradiation.

We are, therefore, proposing qualitative explanations of the fishtail effect, which are consistent with all our experimental data and with data published in the literature. Nevertheless, more detailed theoretical work as well as further experimental studies are necessary to validate some specific assumptions.

ACKNOWLEDGMENTS

The authors wish to thank B. W. Veal, Argonne National Laboratory, K. Winzer, University of Göttingen, M. Murakami, ISTEC Japan, and J. Karpinski, ETH Zürich, for providing us with samples. Special thanks (for their warm hospitality) go to Y. Yeshurun, Bar Ilan University, Tel Aviv, and to R. Griessen, Vrije Universiteit Amsterdam. We also thank H. Niedermaier, Atominstitut Wien, for his expert technical assistance.

[1] H.W. Weber, in *Handbook on the Physics and Chemistry of Rare Earths*, Special Volumes on High Temperature Rare Earth Superconductors, edited by K.A. Gschneidner, Jr., L. Eyring, and M.B. Maple (Elsevier, Amsterdam, in press), Chap. 8.

[2] H. Hillmann and D. Hauck (unpublished).

[3] J.A. Evetts and J.M.A. Wade, J. Phys. Chem. Solids **31**, 973 (1970).

[4] A.I. Larkin and Yu.N. Ovchinikov, J. Low Temp. Phys. **34**, 409 (1979).

[5] R. Meier-Hirmer, H. Küpfer, and H. Scheurer, Phys. Rev. B **31**, 183 (1985).

[6] M. Daeumling, J.M. Seuntjens, and D.C. Larbalestier, Nature (London) **346**, 332 (1990).

[7] A.A. Zhukov, H. Küpfer, S.A. Klestov, V.I. Voronokova, and V.K. Yanovsky, J. Alloys Compd. **195**, 479 (1993).

[8] L.F. Cohen, J.R. Laverty, G.K. Perkins, A.D. Caplin, and W. Assmus, Cryogenics **33**, 352 (1993).

[9] P.A.J. de Groot, Y. Zhu-An, R. Yanru, and S. Smith, Physica C **185**, 2471 (1991).

[10] S.N. Gordeev, W. Jahn, A.A. Zhukov, H. Küpfer, and T. Wolf, Phys. Rev. B **49**, 15 420 (1994).

[11] M. Ullrich, D. Müller, K. Heinemann, L. Niel, and H.C. Freyhardt, Appl. Phys. Lett. **63**, 406 (1993).

[12] Yu.V. Bugoslavsky, A.L. Ivanov, A.A. Minakov, and S.I. Vasyurin, Physica C **233**, 67 (1994).

[13] Yu.V. Bugoslavsky, A.L. Ivanov, and A.A. Minakov, in *Applied Superconductivity*, edited by H.C. Freyhardt (DGM Informationsgesellschaft, Oberursel, 1993), Vol. 1, p. 849.

[14] V. Hardy, A. Wahl, A. Ruyter, A. Maignan, C. Martin, L. Coudrier, J. Provost, and Ch. Simon, Physica C **232**, 347 (1994).

[15] L. Krusin-Elbaum, L. Civale, V.M. Vinokur, and F. Holtzberg, Phys. Rev. Lett. **69**, 2280 (1992).

[16] L. Civale, L. Krusin-Elbaum, J.R. Thompson, and F. Holtzberg, Phys. Rev. B **50**, 7188 (1994).

[17] G. Blatter, M.V. Feigel'man, V.B. Geshkenbein, A.I. Larkin, and V.M. Vinokur, Rev. Mod. Phys. **66**, 1125 (1994).

[18] A. A. Zhukov, H. Küpfer, S. N. Gordeev, W. Jahn, T. Wolf, V. I. Voronkova, A. Erb, G. Müller-Vogt, H. Wühl, H. J. Bornemann, K. Salama, and D. Lee, in *Critical Currents in Superconductors*, edited by H. W. Weber (World Scientific, Singapore, 1994), p. 229.

[19] Y. Yeshurun, E. R. Yacoby, L. Klein, L. Burlachkov, R. Prozorov, N. Bontemps, H. Wühl, and V. Vinokur, in *Critical Currents in Superconductors* (Ref. 18), p. 237.

[20] L. F. Cohen, G. Perkins, A. D. Caplin, A. A. Zhukov, S. A. Klestov, V. I. Voronkova, H. Küpfer, T. Wolf, and S. Abell, in *Critical Currents in Superconductors* (Ref. 18), p. 217.

[21] L.F. Cohen, G. Perkins, A.D. Caplin, S. Abell, A.A. Zhukov, and V.I. Voronkova, Physica C **235-240**, 2885 (1994).

[22] L.F. Cohen, A.A. Zhukov, G. Perkins, H.J. Jensen, S.A. Klestov, and V.I. Voronkova, S. Abell, T. Wolf, and A.D. Caplin, Physica C **230**, 1 (1994).

[23] A.J.J. van Dalen, M.R. Koblischka, R. Griessen, M. Jirsa, and G. Ravi Kumar, Physica C **250**, 265 (1995).
[24] H.G. Schnack, R. Griessen, J.G. Lensink, and Wen Hai-Hu, Phys. Rev. B **48**, 13 178 (1993).
[25] M.R. Koblischka, A.J.J. van Dalen, Th. Schuster, M. Leghissa, and M. Jirsa, Physica C **235-240**, 2839 (1994).
[26] H. Küpfer, Th. Wolf, C. Lessing, A.A. Zhukov, X. Lancon, R. Meier-Hirmer, W. Schauer, and H. Wühl, Phys. Rev. B **58**, 2886 (1998).
[27] H. Küpfer, A.A. Zhukov, A. Will, W. Jahn, R. Meier-Hirmer, Th. Wolf, V.I. Voronkova, M. Kläser, and K. Saito, Phys. Rev. B **54**, 644 (1996).
[28] H. Küpfer, A.A. Zhukov, R. Kresse, R. Meier-Hirmer, W. Jahn, T. Wolf, T. Matsushita, K. Kimura, and K. Salama, Phys. Rev. B **52**, 7689 (1995).
[29] A. Erb, J.-Y. Genoud, F. Marti, M. Däumling, E. Walker, and R. Flükiger, J. Low Temp. Phys. **105**, 1033 (1996).
[30] F.M. Sauerzopf, Phys. Rev. B **57**, 10 959 (1998).
[31] Y. Abulafia, A. Shaulov, Y. Wolfus, R. Prozorov, L. Burlachkov, and Y. Yeshurun, Phys. Rev. Lett. **77**, 1596 (1996).
[32] J. P. Hirth and J. Lothe, *Theory of Dislocations* (Wiley, New York, 1982), Chap. 15.
[33] A. Erb, E. Walker, J.-Y. Genoud, and R. Flükiger, Physica C **282-287**, 89 (1997).
[34] A. Erb, J.-Y. Genoud, M. Dhalle, F. Marti, E. Walker, and R. Flükiger, Appl. Supercond. **158**, 1109 (1997).
[35] T.B. Lindemer, J.F. Hunley, J.E. Gates, Jr., A.L. Sutton, J. Brynestad, C.R. Hubbard, and K.K. Gallagher, J. Am. Ceram. Soc. **72**, 1775 (1989).
[36] M. Werner, Ph.D. thesis, Technical University Vienna, 1997.
[37] J. Karpinski, G.I. Meijer, H. Schwer, R. Molinski, E. Kopnin, K. Conder, M. Angst, J. Jun, S. Kazakov, A. Wisniewski, R. Puzniak, J. Hofer, V. Alyoshin, and A. Sin, Supercond. Sci. Technol. **12**, R1 (1999).
[38] J.-Y. Genoud, A. Erb, B. Revaz, and A. Junod, Physica C **282-287**, 457 (1997).
[39] M. Werner, G. Brandstätter, F.M. Sauerzopf, H.W. Weber, A. Hoekstra, R. Surdeanu, R.J. Wijngaarden, R. Griessen, Y. Abulafia, Y. Yeshurun, K. Winzer, and B.W. Veal, Physica C **303**, 191 (1998).
[40] H. P. Wiesinger, Ph.D. thesis, TU-Wien, 1991.
[41] W. Kritscha, Ph.D. thesis, TU Wien, 1991.
[42] F.M. Sauerzopf, H.P. Wiesinger, H.W. Weber, and G.W. Crabtree, Adv. Cryog. Eng. **38**, 901 (1992).
[43] H.P. Wiesinger, F.M. Sauerzopf, and H.W. Weber, Physica C **203**, 121 (1992).
[44] C.P. Bean, Phys. Rev. Lett. **8**, 250 (1962); C.P. Bean, Rev. Mod. Phys. **36**, 31 (1964).
[45] H. W. Weber and G. W. Crabtree, *Studies of High Temperature Superconductors*, edited by A. V. Narlikar (Nova Science, New York, 1992), Vol. 9, p. 37.
[46] F.M. Sauerzopf, H.P. Wiesinger, and H.W. Weber, Phys. Rev. B **51**, 6002 (1995).
[47] H.W. Weber, H. Böck, E. Unfried, and L.R. Greenwood, J. Nucl. Mater. **137**, 236 (1986).
[48] M.C. Frischherz, M.A. Kirk, J. Farmer, L.R. Greenwood, and H.W. Weber, Physica C **232**, 309 (1994).
[49] M. Aleksa, P. Pongratz, O. Eibl, F.M. Sauerzopf, H.W. Weber, T.W. Li, and P.H. Kes, Physica C **297**, 171 (1998).
[50] M. Werner, F.M. Sauerzopf, H.W. Weber, B.W. Veal, F. Licci, K. Winzer and M.R. Koblischka, Physica C **235-240**, 2833 (1994).
[51] E.H. Brandt, J. Low Temp. Phys. **26**, 709 (1976).